NbN MIXERS AND TUNING CIRCUITS FOR 630 GHz: DESIGN AND PRELIMINARY MEASUREMENTS

M. Salez, J.A. Stern, W.R. McGrath, H.G. LeDuc
Center for Space Microelectronics Technology, Jet Propulsion Laboratory, California Institute of Technology, 4800 Oak Grove Drive, 91109 Pasadena

P. Febvre
DEMIRM-Observatoire de Paris, 61 avenue de l'Observatoire, 75014 Paris, France

ABSTRACT

At frequencies above the gap frequency of niobium (710 GHz), the performance of Nb/AlOx/Nb SIS mixers degrades and the losses in the niobium films of the superconductive Nb/SiO/Nb microstrip circuits used to provide a good RF impedance match severely limit the performance. Therefore, we are investigating the properties of NbN mixers, and in particular of NbN/SiO/NbN microstrip circuits integrated with submicron NbN/MgO/NbN tunnel junctions. The very large penetration depth of NbN (3000-4000 Å) makes the circuit design difficult and also puts critical constraints on alignment during fabrication. We present here the design of several rf tuning circuits for 630 GHz including novel symmetric designs which ease the alignment tolerances. In addition, a new approach for determining experimentally the penetration depth in the NbN films is presented.

I. INTRODUCTION

It has been shown both theoretically and experimentally that SIS mixers work well at frequencies up to the gap frequency of the superconductor used, and less well above that frequency [1-3]. In the case of Nb-based mixers, this frequency is about 710 GHz, the gap frequency of niobium. One reason for this performance degradation is the overlap of photon steps from opposite voltage branches of the tunnel junction's *I-V* curve, which yields a mixer noise increase of up to 50%. This has been investigated with Nb-based mixers from 490 GHz to 650 GHz [4]. Probably, the most impeding factor for the use of SIS mixers above the gap frequency is the exceedingly large rf losses in the superconductive films, as predicted by the Mattis-Bardeen theory. With such high losses, the integrated circuit which should be a purely reactive impedance transformer becomes a highly resistive device dissipating a major fraction of the rf power available to the overall mixer.

A potential solution for building SIS mixers at frequencies above 700 GHz is to use another superconductor with a higher gap energy for the tunnel junction and its integrated tuning circuits. Since NbN has a gap energy about twice as large as that of Nb, NbN-based SIS mixers should in principle work up to 1400 GHz. We are therefore investigating the use of submicron NbN/MgO/NbN tunnel junctions integrated with NbN/SiO/NbN microstrip tuning circuits. The present work focuses on operation near 630 GHz to facilitate the comparison between the well-characterized performance of Nb mixers at this frequency [5] and that of

a similar NbN mixer with identical integrated tuning circuits, when both are used in a waveguide receiver.

II. NbN/SiO/NbN MICROSTRIP TUNING CIRCUITS

A. Circuit Design

NbN films offer the advantage over Nb and lead-alloy films of an energy gap about twice as large, 2Δ=5 meV, so that in theory they become lossy for frequencies higher than 1200 GHz. The fabrication process of NbN/MgO/NbN tunnel junctions has been described elsewhere [6]. The submicron (0.4x0.4 μm^2) tunnel junctions are patterned by electron-beam lithography, while the integrated microstrip circuits are produced by photolithography. The NbN layers are deposited by DC magnetron sputtering, while the MgO barrier layer is produced by rf magnetron sputtering, with an oxygen glow discharge to cure potential pinholes in the barrier. A gold layer is added on top of the counterelectrode layer to avoid oxydation. The penetration depth of the NbN films has been measured via SQUID measurements [7]. It has been found to depend on the temperature of the substrate at the time of deposition. When the substrate is heated to 300 °C during film deposition the transition temperature increases from 14 K to 16 K, with the corresponding penetration depth λ varying from 3800 Å to 2800 Å. For our circuit design calculations, a value of 3200 Å was assumed, and the variations in each design should allow for at least ±300 Å. A critical current density of j_c = 20 kA/cm^2 was chosen for the tunnel junctions, corresponding to $R_n.A$ = 20 $\Omega\mu m^2$. These junctions are characterized by R_n=125 Ω and C=16 fF, yielding $\omega R_n C$ = 7.5 at 600 GHz.

The integrated NbN/SiO/NbN superconductive microstrip circuits have been designed to match these junctions to a typical impedance that the mixer mount should provide, i.e with a real part comprised between 25 Ω and 150 Ω. The transmission line properties have been calculated using the Wheeler formulation [8] for the fringing fields which leads to an effective width, effective characteristic impedance, and effective dielectric constant (see reference [11] for a detailed discussion of the circuit design formulas). We have taken the superconductive behavior of the films into account [9] using an effective permeability μ_{eff} given by:

$$\mu_{eff} = 1 + \lambda/t_d \, (\coth(t_1/\lambda) + \coth(t_2/\lambda)) \qquad (1)$$

where t_d and ε_r are the thickness and dielectric constant of the SiO layer respectively, and t_1 and t_2 are respectively the thickness of the base and top electrodes of the microstrip. All the microstrip circuits use t_1=3000 Å, t_2=5000 Å, t_d=2000 Å, ε_r=5.5, and the normalized propagation velocity v/c varies between 0.195 and 0.215, depending on the width of the microstrip. For certain circuits, the effect of large step discontinuities had to be calculated, using the Oliner inductance formula [10], so as to modify the actual length of a transmission line section to obtain the correct electrical length. The 4μmx4μm pad formed by the wiring layer around the junction adds 4 fF to the junction capacitance. The

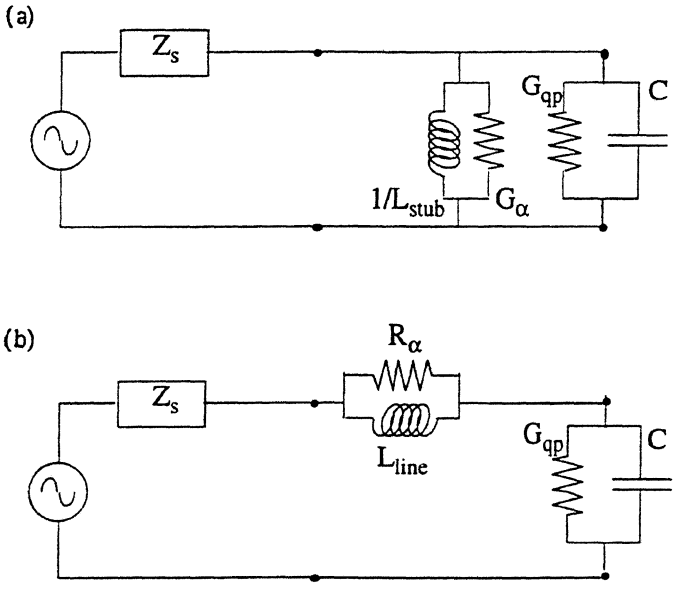

Fig. 1. Schematic diagram of a tunnel junction represented by the admittance $G_{qp} + j.C\omega$, where G_{qp} is the quasiparticle tunneling conductance and C is the geometric capacitance, matched to the source of impedance Z_s with (a) parallel and (b) series tuning circuits. L is the tuning circuit inductance, and G_α and R_α represent resistive losses.

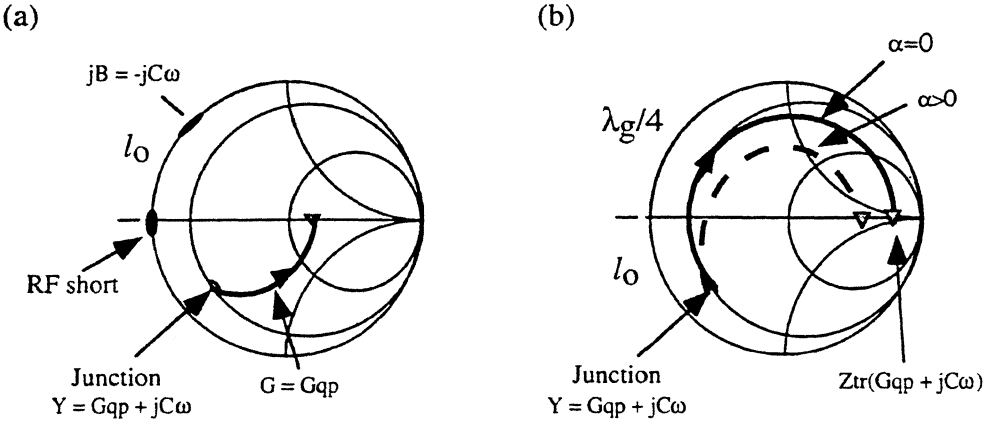

Fig. 2. Illustration on a Smith chart normalized to the source impedance of (a) a parallel tuning circuit and (b) a series tuning circuit, realised by means of distributed elements. In both (a) and (b) l_0 is the length of the section of transmission line required to transform the junction admittance $Y = G_{qp} + jC\omega$ into a purely real load (left on the real axis of the Smith chart). In (a) this is also the length of transmission line that transforms a short (the radial stub) into an admittance whose reactive part jB is the complex conjuguate of the junction susceptance, $jC\omega$. Hence, the junction and the radial stub in parallel have an impedance $1/G_{qp}$. In (b), the low-impedance load produced by the l_0 long transmission line loaded by the junction is further transformed by a $\lambda/4$ section of line into a high-impedance load, easier to match with a waveguide mixer mount. The dashed line indicates the effect of rf losses ($\alpha > 0$).

performance of all the circuits has been evaluated in terms of the return loss at the input of the junction/tuning circuit device, for an assumed source impedance provided by the mixer mount of about 50 Ω.

The circuits can be split in two categories, depending on whether they are parallel circuits or series tranformers (see Fig. 1). The principle of their operation is shown on Smith's charts in Fig. 2 and discussed in more detail below.

Parallel circuits:

Radial stubs. Parallel circuits which provide an inductane in parallel with the junction capacitance have been used for many years. Figure 3(a) shows a microstrip implementation of this type of tuning circuit. A radial stub provides a broadband rf short which is transformed into the proper inductance by a short section of microstrip line (for simplicity, we refer to the stub and microstrip line as a "radial stub" tuning circuit). Both radial stubs and conventional quarter-wave stubs have been used at 600 GHz and have yielded good mixer performance [5, 13]. Radial stubs usually provide the broadest frequency response, around 75 GHz for S_{11}= -10 dB. The difficulty of scaling the radial stub design used with Nb to the NbN material lies in the very short physical lengths associated with the large penetration depth. Errors of only 1 μm in the length of the microstrip line have an enormous effect on the stub response, shifting its central frequency by as much as 30 GHz. A solution to this alignment issue is discussed in II.C below.

Twin-junction transformers. These transformers use two junctions separated by a short section of transmission line, in such a way that the complex impedance of one junction, transformed by the line, acts as a reactive element that exactly compensates for the capacitance of the other [12]. This approach has been used successfully up to 700 GHz [12,14]. Such a transformer must be understood as a parrallel stub of a particular type, which instead of using a broad rf short uses the complex impedance of another junction to provide the inductance $1/\omega C$ that is needed to resonate out C. Because it relies on a highly reactive load (the junction capacitance), it can be expected that these 'stubs' achieve a bandwidth narrower than those using a broadband rf short. The bandwidth is maximized for $Z_C >> R_n$, where Z_C is the characteristic impedance of the transmission line. Calculations show that even for a relatively large junction area (0.8x0.8 μm^2) and narrow line (2 μm), the -10 dB bandwidth is only 40-50 GHz at 600 GHz or about 7%. However, this circuit offers two advantages: First, it requires a smaller area of NbN film since it avoids the need for a wide radial stub or quarter-wave stub. This can be of interest if the losses in NbN films prove to be prohibitive for the use of large stubs. Second, the distance between the two junctions, which determines the amount of induction connected in parallel, does not suffer from possible misalignments as does the section of line linking the junction to the rf short.

Series transformers:

Tchebychev two-pole transformers. These circuits have been used [13,15] and achieve the largest bandwidth. The junction complex impedance is transformed by a short microstrip line of length l_o into a purely resistive load, which is then

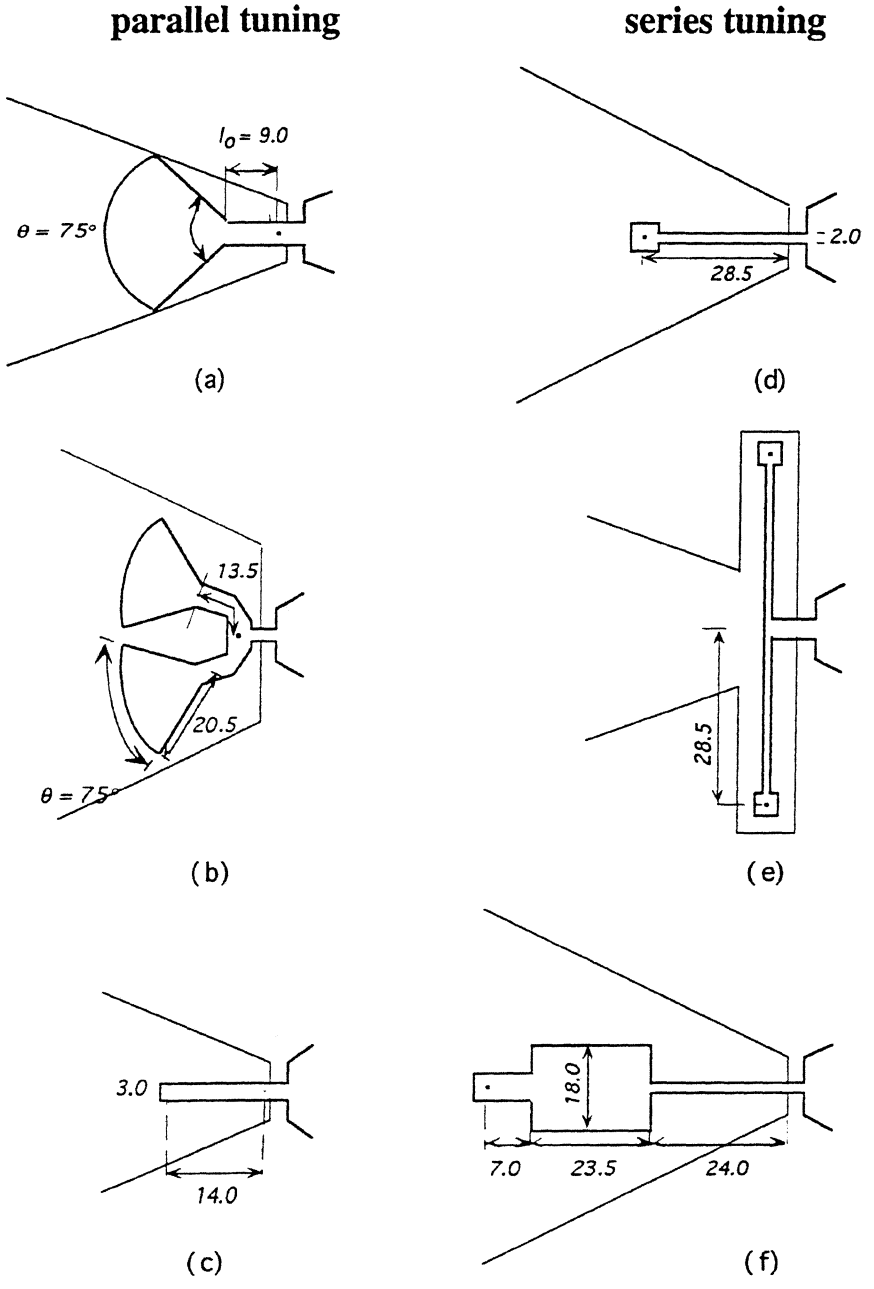

Fig. 3. Summary of the tuning circuits investigated: (a) single radial stub; (b) twin radial stub; (c) twin-junction transformer; (d) single-section transformer; (e) twin single-section transformer; (f) two-section Tchebychev transformer.

transformed to $\approx 50\ \Omega$ by a transformer consisting of two nearly quarter-wave microstrips of well-defined characteristic impedances. As previously discussed [16], the purely real impedance which has to be transformed is extremely small (a few ohms) in the lossless case, which requires a low-impedance (wide) microstrip line as the first $\lambda/4$ section and a large transformation ratio (around 25). The rf losses may improve this situation by increasing the resistance at the transformer input. Our calculations show that S_{11} can be lower than -10 dB over more than 100 GHz bandwidth for small losses ($\alpha=10^{-3}/\mu m$), and up to 200 GHz for moderate losses ($\alpha=10^{-2}/\mu m$). Therefore, even in the worst case, the bandwidth is adequate for many receiver applications, and uncertainties in λ and in the junction capacitance have a negligible effect. Errors in the length of the first section of microstrip line, like those due to misalignments, have also no effect.

Single-section transformers. These are the simplest transformers. They consist of a single section of microstrip line which transforms the junction complex impedance into a purely real impedance in the high impedance region of the Smith's chart (see Figs. 2(b) and 3(d)). The microstrip length is $l_o + \lambda/4$, where l_o is the length defined above. Depending on losses in the microstrip, the value of the impedance varies between 20 and 100 Ω. The -10-dB bandwidth in the lossless case is about 150 GHz.

B. Microwave Losses

Although calculations based on the Mattis-Bardeen theory predict that rf losses in NbN are negligible near 600 GHz, there is experimental evidence [17] that NbN-based microstrip tuning circuits are much lossier than Nb-based ones, perhaps as an effect of grain boundaries in the NbN superconductive films. Hence, in addition to using the Mattis-Bardeen formulas, we have included the rf losses via a range of empirical values for the absorption per unit length. From previous measurements of the quality factor associated with the Josephson resonance seen in the *I-V* curves of NbN tunnel junctions integrated with open-ended stubs in the low-coupling limit induced by a magnetic field, an absorption of about $10^{-2}/\mu m$ has been derived. In our calculations of the tuning circuits properties, we have taken into account absorption factors varying from $10^{-3}/\mu m$ to $10^{-1}/\mu m$. We believe those two numbers to be respectively optimistic and pessimistic values for the range of losses that could occur in the NbN films at 600 GHz.

Two effects of these losses can be distinguished depending on whether one deals with a parallel-type or a series-type impedance transformer. In the parallel circuits, rf losses appear as a parasitic conductance G_α branched in parallel with the junction capacitance and quasiparticle conductance G_{qp}. In the series transformers, rf losses can be modelled by a resistance in series with the junction, which modifies the impedance transformation ratio and cause the power reaching the tunnel junction to be smaller than the power available at the input to the transformer. In the following, the junction parameters are taken to be $R_n=$ 125 Ω and C= 21 fF.

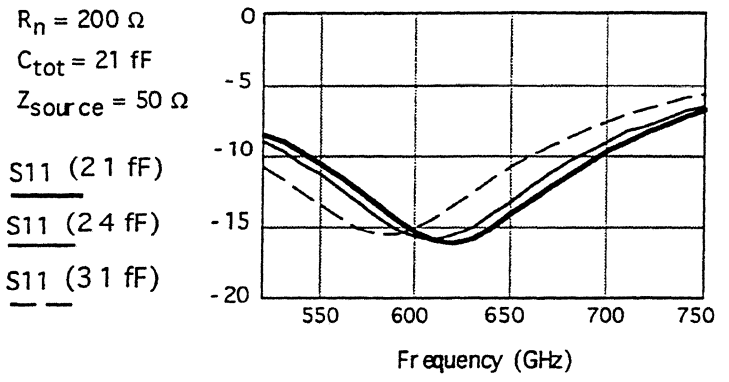

Fig. 4. Reflection coefficient at the input of a single-section end-loaded transformer, for a mixer mount source impedance of Z_S=50 Ω. The different curves show the consequence of errors on the junction capacitance.

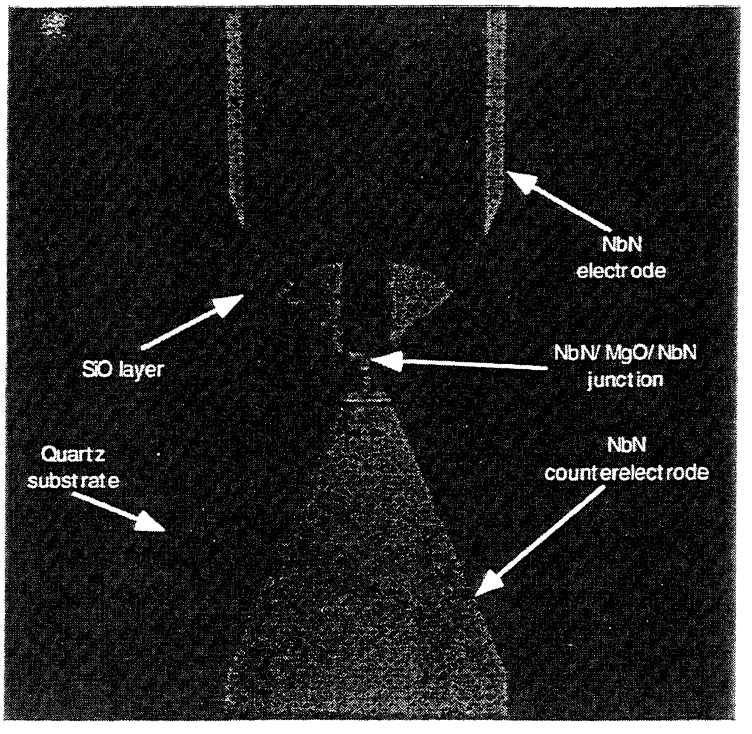

Fig. 5. Photograph of a twin-radial stub.

Parallel stubs. At the resonance frequency of the junction-stub circuit, the input impedance presented by the combination is:

$$Z_{mixer} = 1/(G\alpha + G_{qp}) \qquad (2)$$

In the case of very high losses (α=10^{-1}/μm), $G\alpha$ can be as large as 17 / R_n. This implies about 13 dB loss in the rf power actually coupled into the junction, along

with a real part of the equivalent input impedance as low as 7 Ω. For $\alpha = 5 \times 10^{-3}/\mu m$, the numbers above become 4 dB and 70 Ω. Hence losses in the NbN films can have a substantial effect in terms of an unpredicted mismatch and a large derivation of the rf power away from the quasiparticle nonlinearity. While a suitable amount of tunability of the mixer mount may cope with the former effect, there is no means of avoiding the poor coupling due to the latter effect. The $\alpha=10^{-1}/\mu m$ case which we believe is a more realistic assumption leads to a real impedance of 42 Ω, an impedance easily matched by the mixer mount, and to an additional 6-dB of rf losses, which should not overwhelmingly impede the mixer operation.

Series transformers. The consequences of rf losses in the films are less dramatic here than in the case of parallel tuning. For α between $5 \times 10^{-3}/\mu m$ and $10^{-1}/\mu m$, the equivalent impedance measured at the transformer input varies between 20 Ω and 100 Ω for the single-section transformer, and between 22 Ω and 50 Ω for the Tchebychev transformer. Our waveguide mixer mount is, in theory, capable of matching any real impedance in this range. One notes that the single-transformer is the only tuning circuit that may lead, in the lossless limit, to an impedance possibly too high for the mixer mount to match. Any rf losses then act in a positive way, since it reduces the real part of the transformed impedance as one moves away from the junction to finally intersect the real axis on the Smith chart (see Fig. 2(b)). However, assuming a good impedance match provided by the waveguide mount, rf losses also decrease the fraction of the power coupled into the junction. This fraction can be written

$$\Delta P / P_{in} = 1 - e^{-2\alpha l} \qquad (3)$$

where l is the transformer line length, P_{in} is the power available at the input to the transformer, and ΔP is the power coupled into the junction. Using this simple model, in the case of the single-section transformer, $\Delta P / P_{in} = 0.85$ for $\alpha=10^{-2}/\mu m$ and $\Delta P / P_{in} = 0.92$ for $\alpha=5.10^{-3}/\mu m$. This means that the power loss is smaller than 1 dB for $\alpha<10^{-2}/\mu m$. For higher absorption rates, however, the loss of power in the transformer itself quickly becomes prohibitive. For $\alpha=10^{-1}/\mu m$, the power loss in the tuning circuit reaches 7 dB. In the case of the Tchebychev transformer, the larger size of the tuning circuit makes the effect of α more severe, leading to typical $\Delta P / P_{in} = 0.5$ for $5 \times 10^{-3}/\mu m < \alpha < 10^{-2}/\mu m$. In addition, the whole of the incident power would be dissipated within the microstrip circuit for α around $10^{-1}/\mu m$.

C. Sensitivity to Alignment

Our earlier work at 600 GHz with NbN junctions tuned with NbN/SiO/NbN open-ended microstrip stubs showed that the extreme sensitivity of the frequency response to the stub physical length made the issue of misalignment during photolithography critical. The resonance frequency was measured in the *I-V* curves for several stub physical lengths ranging from 23 μm to 38 μm with

increments of 0.5 μm. The measurements were in good agreement with the predictions of multi-mode resonance theory, and showed the large frequency shift of the resonance per physical length increment. Although radial stubs have broader bandwidths than open-ended stubs, a 1-μm alignment error along the transmission line connected to the radial stub still causes the central frequency to shift by about 30 GHz, which is comparable to the circuit bandwidth.

We solve this problem by introducing into the circuit design a twin-symmetry, rendering them fairly insensitive to alignment errors as large as 2 μm. The idea is to use whenever possible two identical sections of transmission line instead of one, in a geometry such that an excess of electrical length in one section due to misalignment is automatically compensated by an equivalent lack of electrical length in the other section. This principle can be applied to either parallel-type circuits such as the radial stubs (see Fig. 3(b)) or series-type circuits such as the single-section transformers (see fig. 3(e)). Figure 6 shows the effects of misalignment for both a simple radial stub and a twin-radial stub. In the case of the Tchebychev two-section transformer, there is no need for such a symmetric design since the following two quarter-wave sections naturally tend to wash out 1-2 μm alignment errors. Although the bandwidth achievable with the symmetric circuits is reduced, the usefulness lies in the insensitivity to alignment errors, which is critical for NbN.

Figure 3 summarizes all the rf tuning circuits for our NbN mixers. About 5 variations were designed for each to account for variations in junction capacitance and penetration depth.

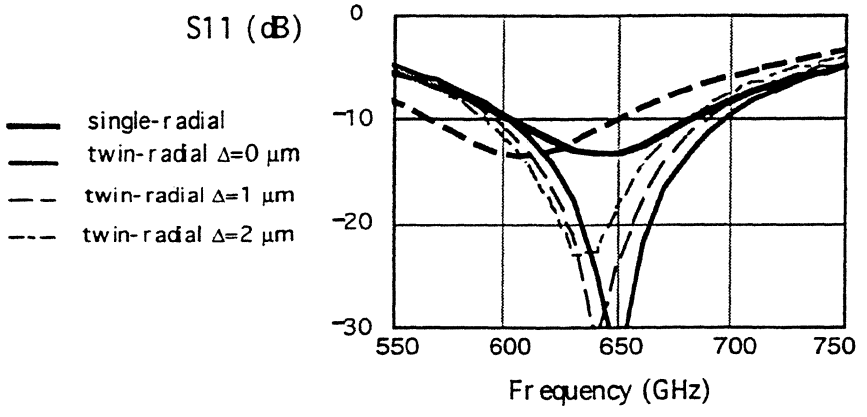

Fig. 6. Compared effects of 1 and 2 μm alignment errors on the tuning achieved by a simple radial stub (heavy lines) and a twin-radial stub (thin lines). The solid curves correspond to a perfect alignment while the dashed curves indicate the frequency-shifted response for a given amount of misalignment.

III. DC MEASUREMENTS

A. Devices Fabricated

One batch of 0.4x0.4 μm^2 NbN/MgO/NbN junctions have been fabricated, with $R_n.A$ around 50 $\Omega.\mu m^2$ and V_{gap}= 4.95 mV. Figure 6 shows one junction integrated with the twin-radial stubs introduced earlier. A typical *I-V* curve is shown in Fig. 7. The corresponding critical current density is 7-10 kA/cm^2. The subgap-to-normal resistance ratio is around 5, and the subgap current is much reduced in comparison with previous batches with higher critical current densities. In particular, a bump-like half-gap feature which appears in all NbN tunnel junctions becomes small at low current densities, which is expected if this feature results from two-particle tunneling in a highly non-uniform oxide barrier [18]. The normal resistance of nearly 200 Ω is higher than the nominal value of 125 Ω assumed for the calculations. However, deviation from the optimum value is less critical for the normal resistance than for the geometric capacitance or the film penetration depth, which drastically modify the length of transmission line required for tuning.

B. Josephson Resonances

The DC characteristics of several circuits have been investigated, and the voltages at which Josephson resonances occur in the *I-V* curves have been measured. From such measurements, it is possible to deduce the frequency at which a parallel tuning stub resonates out the junction's capacitance [13,17]. In the case of a series-type transformer, it is more difficult to correlate the DC Josephson resonance to the actual mixer circuit behavior, since the impedance seen by the tunnel junction is a function of the rf source impedance supplied by the waveguide mount. Two-section Tchebychev transformers, however, can at least tell us at what frequency the two poles resonate, providing information on the rf properties of the superconductive microstrips. Similarly, although the simpler transformers provide little or no information on the propagation velocity in the lines, their symmetric counterparts do. This is because the two end-loaded sections of transmission line make an ideal microstrip resonator ,whose modes can be excited by the AC Josephson currents of each junction at the ends. This microstrip resonator is also a useful feature of the design since it traps additional magnetic flux to cancel the Josephson effect during mixer operation.

The resonances described above have been measured in the radial, twin-radial and twin-transformers (see Fig. 3(a), (b), and (e)). There is good agreement between the resonance frequencies measured in the *I-V* curves and the calculated resonances using the actual $R_n.A$ product and the measured penetration depth. More work needs to be done, however, before an exhaustive comparison between theory and experiment can be made. Twin-radial stubs and twin-transformers have shown DC resonances indicating nominal operation near 500-650 GHz, and these devices are currently being tested.

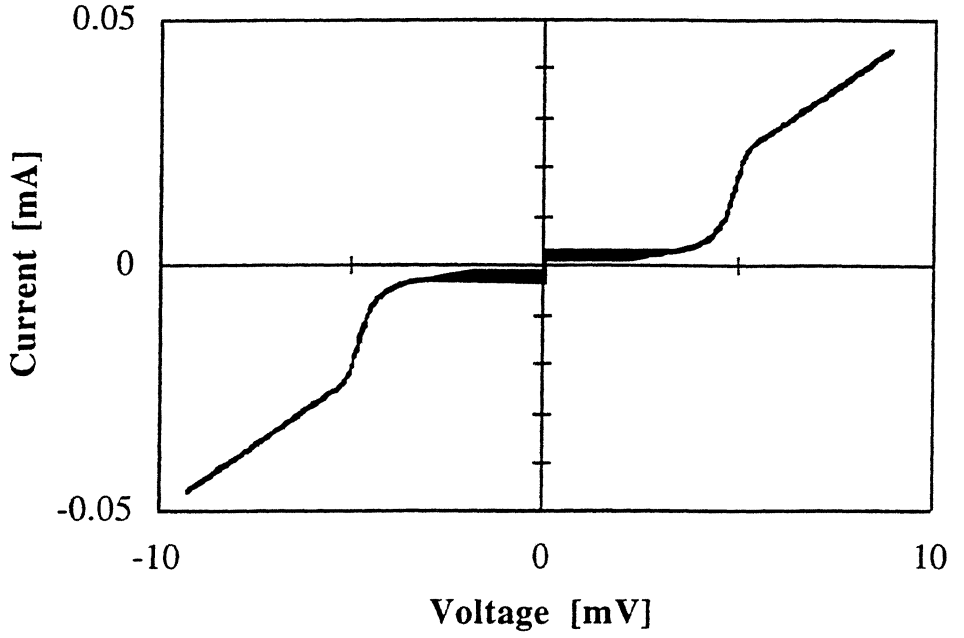

Fig. 7. Measured *I-V* curve of a 0.4x0.4-μm2 NbN/MgO/NbN tunnel junction with $R_n.A$ = 50 Ω.μm2.

C. Penetration Depth Derivation using Long Tunnel Junctions

Accurate values of the penetration depth of the superconductor used for the electrodes of the microstrip circuits is crucial for the design. A well-established method to derive this penetration depth uses the amount of magnetic flux which can penetrate between the two superconductive strips of a SQUID [7]. This method is accurate to ~ 10%. We suggest the use of long (in-line) Josephson junctions (LJJ) to deduce the penetration depth in the superconductive electrodes. A tunnel junction is considered 'long' (see Fig. 8(a)) when its length is several times its width and the Josephson length λ_J, defined as:

$$\lambda_J = (\Phi_O/4\pi\,\mu_O\, j_C\, \lambda)^{1/2} \qquad (4)$$

where Φ_O is the flux quantum and j_C is the critical current density. Then, in the in-line configuration represented in Fig. 8, the density of current flowing through the oxide barrier peaks at the two ends of the LJJ, and decreases toward the center as $e^{-\lambda J}$. Owens and Scalapino [19] have shown that for junctions long enough ($L/\lambda_J > 5$) the maximum supercurrent is independent on the length and is only a function of the critical current density and the junction's width, w:

$$I_{max} = 4w.\lambda_J\, j_C \qquad (5)$$

This maximum supercurrent can be measured with high accuracy in zero magnetic field, allowing the Josephson length to be derived. Equation (4) can then be used to derive λ.

The LJJs not only provide a way to investigate the penetration depth in the films. They also can be used to measure the specific capacitance of the tunnel junctions. It is possible to measure accurately in the *I-V* curves the voltage of the zero-field steps, V_{ZFS}, indicating the resonant motion of flux quanta trapped in the oxide barrier and accelerated by the bias current. Their velocity v is given by

$$v = 2L.V_{ZFS} / \Phi_O \qquad (6)$$

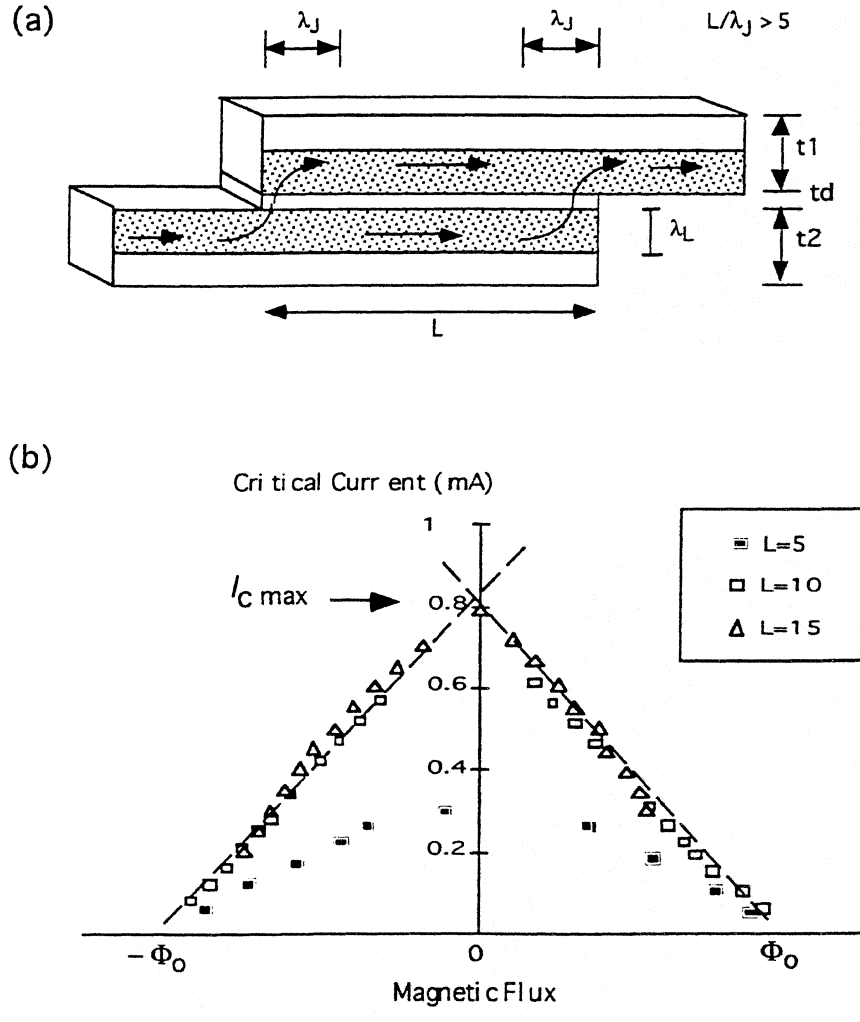

Fig. 8. (a) Schematic drawing of a 'long' Josephson junction showing the confinement of the supercurrent to the edges; (b) measured maximum supercurrent in 5, 10 and 15-μm long junctions versus the applied magnetic flux. Because they are both much longer than the Josephson length (≈2 μm), the 10-μm and the 15-μm junctions are LJJs and hence exhibit the same total supercurrent.

and is also the speed of light in the oxide barrier, of thickness d and of dielectric constant ε_r, that is:

$$v = c\,(d/2\lambda\,\varepsilon_r)^{1/2} \tag{7}$$

Hence by measuring in the same device the penetration depth and the soliton speed, one has also measured the ratio d/ε_r on which depends the specific capacitance of the junction:

$$C/A = \varepsilon_0\,\varepsilon_r/d \tag{8}$$

The *I-V* curves of NbN/MgO/NbN LJJs with w = 0.7, 1 μm, L = 5 , 10 and 15 μm have been measured. The criterion of length is satisfied for L = 10 - 15 μm since $\lambda_J \approx 2.1$ μm, and about the same maximum supercurrent could be measured for junctions of either length. While SQUID measurements have given $\lambda \approx 3500$ Å ±400 Å for NbN, the LJJ method has provided numbers around 3200 Å ± 500 Å. The zero-field steps have been measured in all junctions, giving $v/c \approx 0.018$ and $C/A \approx 90$ fF/μm^2, which is consistent with values deduced previously [7].

This new approach has been tried successfully with NbN and could be used with any other superconductor. The scattering in the method is mostly due to scattering in the measurements of the critical current density in small junctions and of the maximum current in the LJJs, which may occasionally be reduced by trapped flux in the NbN electrodes. This source of scattering disappears with type I superconductors such as Nb.

IV. CONCLUSION

Several NbN/SiO/NbN microstrip rf tuning circuits for NbN-based SIS mixers have been designed, fabricated and will soon be evaluated in a waveguide receiver at 630 GHz. Calculations of these circuits include the effects of fringing fields, strip-width discontinuity, and rf losses in the superconductive films. These circuits take into account design difficulties specifically associated with the potentially higher rf losses in NbN films. Novel symmetric circuits designs have been introduced to address the extreme sensitivity to microfabrication tolerances which result from the long magnetic penetration depth in NbN. In addition, a new method for deriving experimentally the penetration depth of the NbN films using in-line long tunnel junctions has been used and has given results compatible with previous SQUID mreasurements. This method could be used for other superconductors as well.

ACKNOWLEDGEMENTS

This research described in the paper was performed by the Center for Space Microelectronics Technology, Jet Propulsion Laboratory, California Institute of Technology, and was sponsored by the National Aeronautics and Space Administration, Office of Space Access and Technology. Morvan Salez is currently sponsored by the Research Associateship Program of the National Research Council.

REFERENCES

[1] M.J. Feldman, Internat. J. of Infrared and Millimeter Waves **8**, 1287 (1987).

[2] G. DeLange, C.E. Honingh, M.M.T.M. Dierichs, H.H.A. Schaeffer, H. Kuipers, *Proc. 4th Internat. Symp. on Space Terahertz Technology*, p. 41, UCLA, CA (1993).

[3] J. Zmuidzinas, N.G. Ugras, D. Miller, M. Gaidis, H.G. LeDuc, and J.A. Stern, ASC'95, Boston, MA (1994).

[4] P. Febvre, M. Salez, W.R. McGrath, B. Bumble, and H.G. LeDuc, to appear in Applied Physics Letters (1995).

[5] M. Salez, P. Febvre, W.R. McGrath, B. Bumble, H.G. LeDuc, Internat. J. of Infrared and Millimeter Waves **15**, (6) 349 (1994).

[6] J.A. Stern, B.D. Hunt, H.G. LeDuc, A. Judas, W.R. McGrath, S.R. Cypher, and S.K. Khanna, IEEE Trans. on Magn., **25**, 2, 1054 (1989)

[7] J.A. Stern and H.G. LeDuc, IEEE Trans. on Magn., **27**, 2, 3196 (1991)

[8] H.A. Wheeler, IEEE Trans. Microwave Theory Tech., **MTT-25**, 631 (1977)

[9] J.C. Swihart, 1961, J. Appl. Phys. **32**, 441 (1961).

[10] A.A. Oliner, IRE Trans. Microwave Theory Tech., **MTT-3**, 134, (1955)

[11] P. Febvre, W.R. McGrath, B. Bumble, H.G. LeDuc, S. George, G. Ruffie, G. Beaudin, Proceedings of the 24th. European Microwave Conference, Palais des Festivals, Cannes, France, September 5-8, 1994.

[12] V.Yu. Belitzky, M.A. Tarasov, S.A. Kovtonjuk, L.V. Filippenko, and O.V. Kaplunenko, Internat. J. of Infrared and Millimeter Waves **13**, 389 (1992)

[13] P. Febvre, W.R. McGrath, P. Batelaan, B. Bumble, H.G. LaDuc, S. George, and P. Feautrier, Internat. J. of Infrared and Millimeter Waves **15**, 943 (1994)

[[14] J. Zmuidzinas, H.G. LeDuc, J.A. Stern, and S.R. Cypher, IEEE Trans. Microwave Theory Tech., **42**, 698 (1994)

[15] R. Blundell, C. Tong, J.W. Barett, R.L. Leombruno, S. Paine, D.C. Papa, X. Zhang, J.A. Stern, H.G. LeDuc, and B. Bumble, Proceedings of the European SIS User Meeting, KOSMA, Koln, Germany (1994)

[16] J.W. Kooi, M. Chan, B. Bumble, H.G. LeDuc, P.L. Schaeffer, and T.G. Phillips, Internat. J. of Infrared and Millimeter Waves **15**, 783 (1994)

[17] W.R. McGrath, J.A. Stern, H.H.S. Javadi, S.R. Cypher, B.D. Hunt, and H.G. LeDuc, IEEE Trans. Mag., **MAG-27**, 2650 (1991)

[18] J.R. Schrieffer and J.W. Wilkins, Phys. Rev. Lett., **10**, 17 (1962)

[19] C.S. Owens and D.J. Scalapino, Phys. Rev., **164**, 538 (1967)